High-Resolution Measurement of Fine Structure in the Photoabsorption Cross Section of ^{18}O

H. Harada,[1] Y. Shigetome,[1] H. Ohgaki,[2] T. Noguchi,[2] and T. Yamazaki[2]

[1]*Power Reactor and Nuclear Fuel Development Corporation, Tokai-mura, Ibaraki-ken, 319-11, Japan*

[2]*Electrotechnical Laboratory, 1-1-4 Umezono, Tsukuba-shi, Ibaraki-ken, 305, Japan*

(Received 4 August 1997)

A new experimental method for the high-resolution measurement of photoabsorption cross sections has been developed. The energy resolution of about 0.1% is achieved by measuring the transmitted photons from a target with a high-resolution high-energy photon spectrometer. The method is applied to the measurement of the photoabsorption cross section of ^{18}O in the giant resonance region. Significant fine structure of the resonance is observed. [S0031-9007(97)04928-4]

PACS numbers: 25.20.Dc, 27.20.+n, 29.30.–h

The fine structure in photonuclear reaction cross sections, such as that observed in oxygen [1–5] and other light nuclei [6–8] in the giant resonance (GR) region, can provide important information for the understanding of the GR. In particular, the intrinsic width of the fine peak in the GR region is important because it gives information on the configuration of the resonance. Theoretical approaches reproduce only the position and strength of the peaks and do not account for the width [9–13]. The width has been treated just as a free parameter to fit the experimental data [9]. In some light nuclei, the widths of the levels in the GR region are deduced from the data of the (e, e'), (p, γ), and (α, γ) reactions; the value of the total level width ranges from a few keV to a few hundred keV [14–16]. However, the energy resolution of the photonuclear cross section measurements using tagged photons or monochromatic photons is typically a few hundred keV [17–19] and is, therefore, not enough to deduce the intrinsic width. The high-resolution high-energy photon spectrometer (HHS) was constructed at the Power Reactor and Nuclear Fuel Development Corp. (PNC) to investigate the fine structure of photonuclear reaction cross sections [20]. The HHS was designed to measure high-energy photons, typically 10–30 MeV, with an energy resolution of about 0.1% and with high photopeak-to-background (= total-photopeak) ratio.

The high-resolution measurement using HHS needs no monochromatic photon beams in contrast to the foregoing measurement methods, but white photon beams whose energy covers the fine structure peaks of interest. By counting the transmitted white photons from a target with HHS, the photoabsorption cross section is deduced [20]. For the transmitted photon counting method, the use of laser compton photons (LCP's) [21,22] is more effective [23] than that of bremsstrahlung photons because of its hardness on energy distribution and its energy selectivity.

The HHS (Fig. 1) consists of two large *N*-type Ge detectors and thick bismuth germanium oxide (BGO) detectors surrounding the Ge detectors. The sensitive volume of two Ge crystals is 668 cm^3. The relative efficiency of each detector was 95% at 1.33 MeV relative to a 3 in. diam × 3 in. NaI detector and the energy resolution of each Ge detector was 2.2 keV FWHM at 1.33 MeV. The two Ge crystals are arranged like twins along a beam axis to obtain large photopeak efficiency for high-energy photons. Signals from the two Ge detectors are summed by a high gain-stability sum amplifier. The energy resolution of the twins used in the summed mode was 12 keV FWHM (0.13%) for 9.04 MeV photons generated via a $^{113}Cd(n, \gamma)$ reaction. This performance on energy resolution for high-energy photons is almost the same as that reported for a small Ge(Li) detector [24]. To improve the twin peak/background ratio, the BGO detectors work as an anticoincidence spectrometer [20,25] with the discriminator set at about 100 keV. A beam window of 3 cm diameter is provided in the front BGO detector.

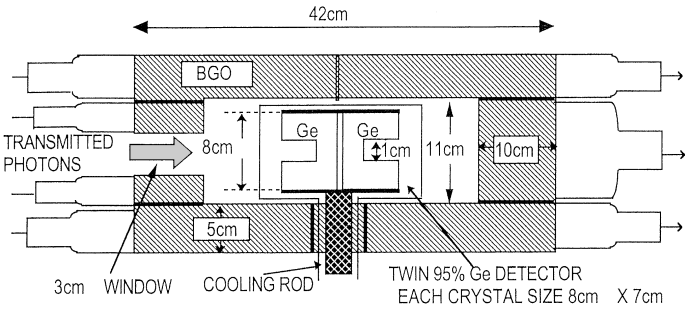

FIG. 1. A schematic representation of the HHS.

The HHS was designed using the Monte Carlo electron-gamma shower simulation code, EGS4 [26]. According to the simulation, the absolute photopeak efficiency of HHS is 6.5% for a collimated 15 MeV photon beam of 2 cm diameter.

The experiment was performed at the electron storage ring TERAS [27,28] of Electrotechnical Lab (ETL). The experimental arrangement is shown in Fig. 2. A second harmonics of yttrium lithium tetrafluoride laser beam ($\lambda = 527$ nm and the power 1–3 W) entered the window of a vacuum chamber inside the bending magnet after being reflected by a mirror and passing through a lens ($f = 2.0$ m), and then interacted with the stored electron beam at the straight section. The energy of the stored electron beam was 615 MeV and the stored current was 15–150 mA. The maximum energy of the LCP's was 13.4 MeV in this case. The lead collimator of 150 mm in length and with a hole of 5.0 mm diameter was placed along the LCP beam axis to cut off the low energy tail of the LCP beam. The distance between the centers of the interaction region and the collimator was 5.2 m.

The ^{18}O target consisted of an acrylic cylinder of 602 mm in inner length and 11 mm in inner diameter, filled with $H_2{}^{18}O$ enriched to 98% in ^{18}O. A ^{16}O target of the same size was also prepared for the comparison of the transmitted spectrum of ^{16}O with that of ^{18}O; the difference of the spectra clearly shows the difference between the photonuclear cross section of ^{18}O and that of ^{16}O because the photon-atom cross sections are the same for the isotopes. The photoabsorption cross section of ^{16}O can be deduced from the data of the $^{16}\mathrm{O}(e, e')$, $^{15}\mathrm{N}(p, \gamma_0)$, and $^{12}\mathrm{C}(\alpha, \gamma_0)$ reactions [15]. Both of the targets were set, in parallel to the LCP beam, on the pulsed-motor driven X stage. The X stage was controlled to change the targets at an interval of 100 sec via the CAMAC controlling system. The summed signals of the two Ge detectors were transferred to an analog-to-digital converter (Canberra 450 MHz model 8077) that was gated by twin-BGO anticoincidence signals. The pulse height data with 8k channels were stored in a hard disk of a personal computer at the interval synchronized with the movement of the ^{16}O and ^{18}O targets.

Figure 3(a) shows the transmitted photon spectra, $Y(^{16}\mathrm{O})$ (■) and $Y(^{18}\mathrm{O})$ (○), observed by HHS for the ^{16}O and ^{18}O targets, respectively. Each spectrum was obtained by summing 837 spectra and packing 50 channels into one channel to present the data with high statistics. Figure 3(b) shows the subtracted spectrum, $Y(^{16}\mathrm{O}) - Y(^{18}\mathrm{O})$. Significant fine structure is shown at the region of $\sim 8-13$ MeV. The gross feature of the fine structure agrees with the previous data [3,4,16], where the only

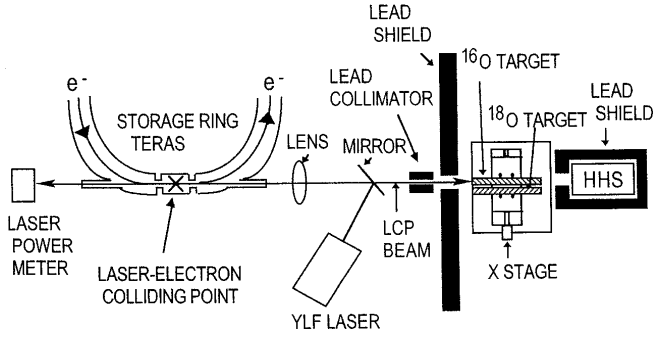

FIG. 2. Schematic overview of the photonuclear experimental area at the LCP facility. The HHS is set along the LCP beam axis.

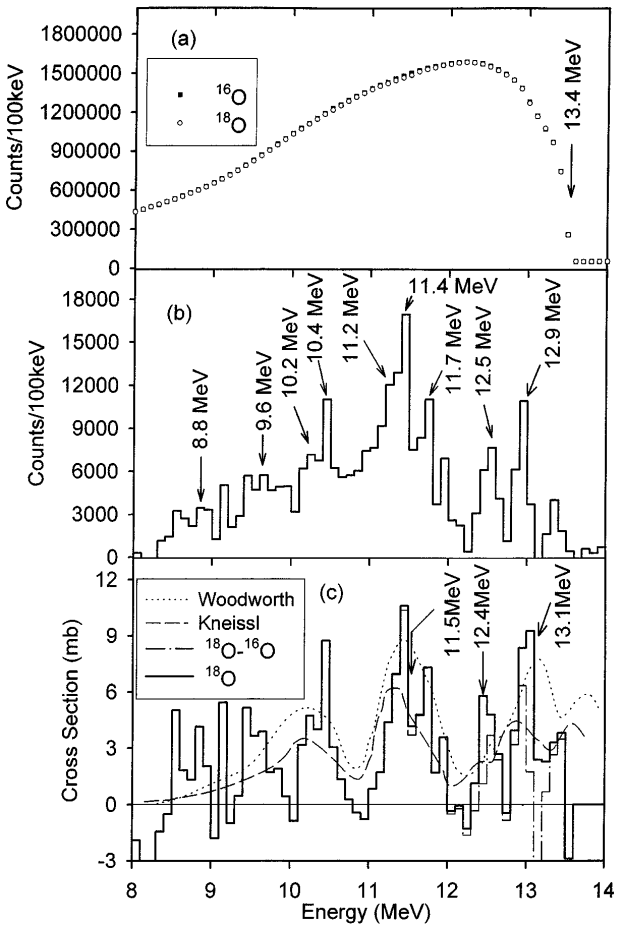

FIG. 3. (a)Transmitted photon spectra from ^{16}O (■) and ^{18}O (○) targets observed by the HHS. (b) Difference of the transmitted spectra, $Y(^{16}\mathrm{O}) - Y(^{18}\mathrm{O})$. Peaks in the range of $\sim 8-13.4$ MeV are due to photonuclear reactions by ^{18}O because the contribution of the photon-atom cross section is canceled out in the subtracted spectrum. Photonuclear cross section of ^{16}O contributes to make negative peaks. (c) Photoabsorption cross section of ^{18}O in the energy range of $\sim 8-13.4$ MeV. The difference of the photoabsorption cross section, $\sigma_{\mathrm{abs}}(^{18}\mathrm{O}) - \sigma_{\mathrm{abs}}(^{16}\mathrm{O})$, is shown by the dash-dotted line. The dashed and dotted lines show the data of Kneissl *et al.* [3] and Woodworth *et al.* [4]. The solid line in (c) shows the photoabsorption cross section of ^{18}O where the contributions of the three dip peaks of ^{16}O are corrected using the values of the total width and the radiative width given in Ref. [15].

four resonances were reported at 9.1, 10.3, 11.4, and 13.1 MeV. The present data resolves the four resonances into nine resonances. For example, the 11.4 MeV resonance is resolved into 11.2, 11.4, and 11.7 MeV resonances. The three resonances are seen in the (γ, n_0) and (γ, n_1) transitions measured by the photoneutron time-of-flight measurements of Ref. [2], but have not been resolved in the (γ, total) cross section measurements [3,4].

The difference of the photoabsorption cross sections, $\sigma_{\rm abs}(^{18}{\rm O}) - \sigma_{\rm abs}(^{16}{\rm O})$, is given by

$$1 - \exp\{-\rho\iota[\sigma_{\rm abs}(^{18}{\rm O}) - \sigma_{\rm abs}(^{16}{\rm O})]\} = [U(^{16}{\rm O}) - U(^{18}{\rm O})]/U(^{16}{\rm O}), \quad (1)$$

where σ and ι are, respectively, the atomic density of ^{16,18}O and the length of the ^{16,18}O target. When $\rho\iota\sigma_{\rm abs} \ll 1$, Eq. (1) is approximated by

$$\sigma_{\rm abs}(^{18}{\rm O}) - \sigma_{\rm abs}(^{16}{\rm O}) \doteqdot [U(^{16}{\rm O}) - U(^{18}{\rm O})]/U(^{16}{\rm O})/\rho\iota. \quad (2)$$

The U in Eqs. (1) and (2) is obtained by unfolding the observed spectrum Y with the response functions of HHS. The response functions of HHS were calculated using the EGS4 simulation code [23]. Here, the U represents the energy distribution of the transmitted photons.

The difference of the photoabsorption cross section, $\sigma_{\rm abs}(^{18}{\rm O}) - \sigma_{\rm abs}(^{16}{\rm O})$, deduced by Eq. (2) is shown by the dash-dotted line in Fig. 3(c). The dashed and dotted lines show the data of Kneissl *et al.* [3] and Woodworth *et al.* [4]. It is expected that there are three large photoabsorption peaks in ^{16}O in the energy region 8–13.4 MeV that have been measured via the $^{16}{\rm O}(e, e')$, $^{15}{\rm N}(p, \gamma_0)$, and $^{12}{\rm C}(\alpha, \gamma_0)$ reactions [15]. The excitation energies of the peaks of ^{16}O are 11.52, 12.44, and 13.09 MeV. The solid line in Fig. 3(c) shows the photoabsorption cross section of ^{18}O where the contributions of the three dip peaks of ^{16}O are corrected using the values of the radiation widths and the total widths of these levels given in Ref. [15]. The spectrum in Fig. 3(c) clearly shows the fine structure of ^{18}O as well as that in Fig. 3(b). The largest correction at 13.09 MeV shifted the peak energy from 12.9 MeV in Fig. 3(b) to 13.0 MeV in Fig. 3(c). For the peaks at 10.4, 11.4, 12.5, and 13.0 MeV in Fig. 3(c), the peak cross section values are larger than those of Refs. [3] and [4]. It is also important to note that the widths of the observed peaks are much narrower than previous data [3,4,16]. These data are summarized in Table I along with the values of Ref. [16] for comparison. The peak cross section σ and the total width $\Gamma_{\rm tot}$ are not presented for the 8.8 and 9.6 MeV peaks because of their poor statistics. There is no experimental systematic uncertainty in the determination of beam current, detector efficiency, background subtraction, and reaction losses in contrast to previous measurements [3,4] because Eq. (2) requires only the ratio between the unfolded HHS spectrum of the ^{18}O target and that of the ^{16}O reference target. Uncertainty in the simulation of the HHS's response functions contributes to the systematic uncertainty of the photoabsorption cross section with magnitudes up to 20%. Statistical uncertainty contributes to the error of the cross section with ~ 0.8–1.1 mb in the region of ~ 10–13 MeV and ~ 1.1–1.8 mb in the region of ~ 8–10 MeV.

The measurement using HHS and LCP resolved four resonance peaks into nine resonance peaks in the regions ~ 8–13.4 MeV. It was found that the widths of resonance peaks at 10.2, 10.4, 11.2, 11.4, 11.7, 12.5, and 13.0 MeV of the ^{18}O target are much narrower than those measured using a quasimonoenergetic photon beam from positron annihilation in flight [3,4]. However, the high-resolution performance of HHS cannot be fully exploited due to limited statistics of the HHS spectra and moderate sharpness of the fine structure peaks observed in ^{18}O. Higher statistics data have the possibility to show the intrinsic shape of the fine structure that should be compared to microscopic studies of the resonances [13]. When the new measurement method of photoabsorption cross section using HHS and LCP is applied to a number of nuclei, it will be a sound experimental basis for the study of fine structure in photoabsorption cross section. The energy resolution of this measurement is more than 10 times superior to that achieved by previous measurements [1–8,17–19].

TABLE I. Resonances in $^{18}{\rm O} + \gamma$.

This expt.			Previous data [26]		
Ex (MeV)	σ (mb)	$\Gamma_{\rm tot}$ (MeV)[a]	Ex (MeV)	σ (mb)	$\Gamma_{\rm tot}$ (MeV)
8.8	...	...			
9.6	...	...	9.1	1.1	0.6
10.2	5	0.1			
10.4	9	0.1	10.3	5.3	0.9
11.2	4	0.1			
11.4	11	0.1	11.4	9.0	0.7
11.7	7	0.1			
12.5	6	0.1			
13.0	9	0.1	13.1	8.6	0.7

[a]Observed width. The experimental resolution is 0.1 MeV.

A straightforward application will be a pair of ^{13}C and ^{12}C (reference target), and a pair of ^{26}Mg and ^{24}Mg (reference target), where fine structures are well known [7,8]. The energy resolution of 0.1% of this measurement will be achieved by observing the photon attenuation in the ^{13}C target where the narrow level width (5.49 keV) is known at the excitation energy of 15.11 MeV. It is, in principle, possible to plan the experiment using a blank target as a reference target, assuming the photon attenuation in the target due to the photon-atom cross section is precisely simulated by the Monte Carlo method. A detailed study of the simulation will enable the photoabsorption cross section measurement for many kinds of targets.

Suggestions of I. Satoh, N. Sasao, S. Yoshida, Y. Torizuka, and J. Kasagi, and valuable discussions starting in the very early stage of the experiment are gratefully acknowledged. We thank S. Nakajima for his help in data analysis. The experimental success would have been impossible without the cooperative effort of the members of ETL accelerator group. This work has been supported by PNC and ETL.

[1] B. S. Dolbilkin *et al.,* Pis'ma Zh. Eksp. Teor. Fiz. **1**, 47 (1965).
[2] J. D. Allan *et al.,* Can. J. Phys. **53**, 786 (1975).
[3] U. Kneissl *et al.,* Nucl. Phys. **A272**, 125 (1976).
[4] J. D. Woodworth *et al.,* Phys. Rev. C **19**, 1667 (1979).
[5] D. Zubanov *et al.,* Phys. Rev. C **45**, 174 (1992).
[6] B. W. Thomas *et al.,* Nucl. Phys. **A196**, 89 (1972).
[7] J. W. Jury *et al.,* Phys. Rev. C **19**, 1684 (1979).
[8] S. C. Fultz *et al.,* Phys. Rev. C **4**, 149 (1971).
[9] C. M. Shakin and W. L. Wang, Phys. Rev. Lett. **26**, 902 (1971).
[10] S. Adachi and S. Yoshida, Nucl. Phys. **A306**, 53 (1978).
[11] G. F. Bertsch *et al.,* Rev. Mod. Phys. **55**, 287 (1983).
[12] H. R. Kissener *et al.,* Fortschr. Phys. **35**, 277 (1987).
[13] S. Kamerdzhiev and J. Speth, Nucl. Phys. **A599**, 373C (1996).
[14] F. Ajzenberg-Selove, Nucl. Phys. **A523**, 1 (1991).
[15] D. R. Tilley *et al.,* Nucl. Phys. **A565**, 1 (1993).
[16] D. R. Tilley *et al.,* Nucl. Phys. **A595**, 1 (1995).
[17] S. V. Springham *et al.,* Nucl. Phys. **A517**, 93 (1990).
[18] J. R. M. Annand *et al.,* Phys. Rev. Lett. **71**, 2703 (1993).
[19] B. L. Berman and S. C. Fultz, Rev. Mod. Phys. **47**, 713 (1975).
[20] H. Harada and Y. Sigetome, J. Nucl. Sci. Technol. **32**, 1189 (1995).
[21] T. Yamazaki *et al.,* IEEE Trans. Nucl. Sci. **32**, 3406 (1985).
[22] H. Ohgaki *et al.,* Nucl. Instrum. Methods Phys. Res., Sect. A **353**, 384 (1994).
[23] J. Kasagi (private communication).
[24] F. E. Cecil *et al.,* Nucl. Instrum. Methods Phys. Res., Sect. A **234**, 479 (1985).
[25] C. Michel *et al.,* Nucl. Instrum. Methods Phys. Res., Sect. A **251**, 119 (1986).
[26] W. R. Nelson *et al.,* SLAC Report No. 265, 1985.
[27] T. Tomimasu *et al.,* IEEE Trans. Nucl. Sci. **30**, 3133 (1983).
[28] S. Sugiyama *et al.,* in *Proceedings of the 9th Symposium on Accelerator Science and Technology* (KEK, Tsukuba-shi, Japan, 1993), pp. 47–49.